Theoretical Modeling of the Oxidation of Hydrazine by Iron(II) Phthalocyanine in the Gas Phase. Influence of the Metal Character

Gloria I. Cárdenas-Jirón,*,† Verónica Paredes-García,*,§ Diego Venegas-Yazigi,|| José H. Zagal,‡ Maritza Páez,‡ and Juan Costamagna‡

Laboratorio de Química Teórica, Departamento de Ciencias Químicas, and Departamento de Química de los Materiales, Facultad de Química y Biología, Universidad de Santiago de Chile (USACH), Casilla 40, Correo 33, Chile, Facultad de Ciencias Naturales, Matemáticas y del Medio Ambiente, Universidad Tecnológica Metropolitana, Av. José Pedro Alessandri 1242, Chile, and CIMAT, Facultad de Ciencias Químicas y Farmacéuticas, Universidad de Chile, Casilla 233, Santiago, Chile

Received: January 31, 2006; In Final Form: August 4, 2006

The hydrazine oxidation by iron(II) phthalocyanine (Fe(II)Pc) has been studied using an energy profile framework through quantum chemistry theoretical models calculated in the gas phase at the density functional theory B3LYP/LACVP(d) level. We applied two models of charge-transfer mechanisms previously reported (*J. Phys. Chem. A* **2005**, *109*, 1196) for the hydrazine oxidation mediated by Co(II)Pc. Model 1 consists of an alternated loss of one electron and one proton, involving anionic and neutral species. Model 2 considers an alternated loss of two electrons and two protons and includes anionic, neutral, and cationic species. Both applied models describe how the charge-transfer process occurs. In contrast with the obtained results for Co(II)Pc, we found that the hydrazine oxidation mediated by Fe(II)Pc is a fully through-bond charge-transfer mechanism. On the other hand, the use of different charge-transfer descriptors (spin density, electronic population, condensed Fukui function) showed a major contribution of the iron atom in comparison with the cobalt atom in the above-mentioned process. These results could explain the higher catalytic activity observed experimentally for Fe(II)Pc in comparison with Co(II)Pc. The applied theoretical models are a good starting point to rationalize the charge-transfer process of hydrazine oxidation mediated by Fe(II)Pc.

1. Introduction

Research in the application of metallophthalocyanine (M−Pc) as catalyst in electro-oxidation and electro-reduction of small molecules has attracted much interest over the past decades, especially because of the practical and industrial applications.[1−6] Modified electrodes with different M−Pc are used as catalyst in a vast number of electrochemical reactions such as H_2O_2,[7] SO_2,[8] hydrazine,[9] and cysteine[10] oxidation. The study of hydrazine and their derivatives has led to several applications as corrosion inhibitors, antioxidants, reducing agents, plant growth regulators, explosives, rocket propellants, and fuel cells.[11] Literature data show several experimental studies of the catalytic activities of different metallophthalocyanines on the electro-oxidation of the hydrazine.[9,12−25] The catalytic activity depends on the nature of the metal ion included in this macrocycle system.[4,26−28] For example, for the electro-oxidation of hydrazine with modified electrodes with different metallophthalocyanines, Zagal et al. have proposed that the catalytic activity decreases in the following order: FePc > CoPc > CuPc ≈ NiPc > graphite.[9] The authors also found that the nature of the metal ion not only determines the activity, but it also determines the mechanisms involved in this oxidation process.

For the reasons mentioned above, theoretical studies on different electro-oxidation or electro-reduction processes are a fundamental tool to rationalize the mechanism of how these processes occur. Two main charge-transfer mechanisms have been previously proposed, a through-bond charge-transfer mechanism (TBCT) and a through-space charge-transfer mechanism (TSCT).[29] Through-bond electron transfer is defined as an intramolecular electron transfer for which the relevant electronic interaction between the donor and acceptor sites is mediated by through-bond interaction, that is, via the covalent bonds interconnecting these sites, as opposed to through-space interaction.[30] The latter (TSCT) is defined as an electron transfer for which the relevant electronic interaction between the donor and acceptor sites is mediated either by direct orbital overlap or by superexchange interaction via intervening molecular entities not covalently bound to the donor or acceptor sites.[30] These concepts have been applied at experimental and theoretical levels.[31]

To identify which charge-transfer mechanism is involved in the four-electron oxidation of hydrazine mediated by Fe(II)Pc, we applied the same methodology previously reported.[29] We present a theoretical study of the oxidation of hydrazine mediated by iron(II) phthalocyanine in the gas phase, and we investigate the influence of the metal center (iron) on the oxidation process. At the experimental level, the difference in the catalytic activity between Fe(II)Pc and Co(II)Pc is known. The present work was performed using the density functional theory (DFT) and applies as a starting point two different oxidation mechanisms previously reported for Co(II)Pc.

2. Computational Details

The molecular geometries of iron(II) phthalocyanine (Fe(II)-Pc), the hydrazine residue ($[N_2H_3]^-$) (Figure 1), and the formed

* Corresponding authors. E-mail: gcardena@lauca.usach.cl (G.I.C.-J.); vpg@manquehue.net (V.P.-G.).
† Departamento de Ciencias Químicas, Universidad de Santiago de Chile.
‡ Departamento de Química de los Materiales, Universidad de Santiago de Chile.
§ Universidad Tecnológica Metropolitana.
|| Universidad de Chile.

10.1021/jp060647r CCC: $33.50
Published on Web 10/04/2006

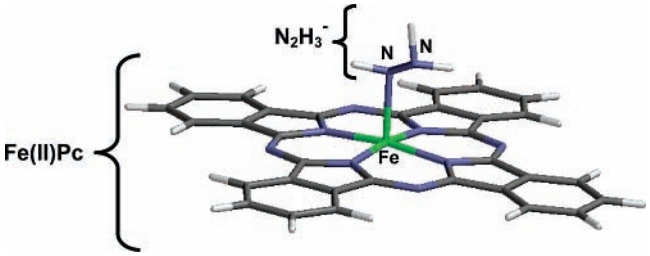

Figure 1. Molecular structures of iron(II) phthalocyanine (Fe(II)Pc) and the anionic hydrazine species ($[N_2H_3]^-$).

adducts between these species were fully optimized by DFT with the B3LYP exchange correlation functional.[32−34] We considered the Becke's three-parameter hybrid exchange functional, which includes the exact Hartree−Fock, Slater, and Becke exchanges, and the Vosko, Wilk, and Nusair local correlation functional and the LYP nonlocal correlation functional. All DFT calculations performed with the TITAN package[35] used the LACVP(d) basis set, which includes an effective core potential with d orbitals for the iron atom and a 6-31G(d) basis set for the lighter atoms such as carbon, nitrogen, and hydrogen. For all of the open shell (RO) systems, a restricted open formalism (ROB3LYP) was used. We propose the use of two models of mechanisms for the hydrazine oxidation. We constructed energy profiles for the different stages of the oxidation process, starting from the interaction Fe(II)Pc + $N_2H_3^-$ and ending with the molecular nitrogen (N_2) release. In these profiles, we have only considered the minimum energy states. Atomic spin densities (ρ^s) and atomic electronic populations (ρ) were analyzed for all of the species, and these properties were used as criteria to determine when the charge transfer occurs. The spin density ($\rho^s(r)$) is defined as the difference in the electronic density formed by electrons with α spin ($\rho^\alpha(r)$) and the electronic density formed by electrons with β spin ($\rho^\beta(r)$), that is, $\rho^s(r) = \rho^\alpha(r) - \rho^\beta(r)$. These spin densities are transformed into atomic spin densities ρ^s using the partition scheme of the electronic density given by NAO (Natural Atomic Orbital),[36−41] which is included in the TITAN package.[35] The latter scheme was also applied to obtain the atomic electronic populations.

Condensed Fukui functions were also used to identify the oxidation sites in the species participating in the mechanism of hydrazine oxidation, as an additional criterion that complements the information obtained by ρ^s and ρ.

3. Results and Discussion

3.1. Through Space−Through Bond. Generally, the experimental electro-oxidation process of hydrazine (N_2H_4) to molecular nitrogen mediated by metal−phthalocyanine is carried out in a strong basic media.[9,12,25,42−44] On the basis of this fact and of other experimental results[12,42] showing the existence of the $[N_2H_3]^-$ species in strong basic media, we used this species as a starting point in the modeling of the oxidation of hydrazine mediated by Fe(II)Pc.

In this work, we studied the oxidation of hydrazine mediated by Fe(II)Pc using the two previously proposed models (models 1 and 2) for the hydrazine oxidation mediated by Co(II)Pc.[29c] In both models, the first step considers the interaction between Fe(II)Pc and the anionic hydrazine species ($[N_2H_3]^-$).

In general terms, model 1 considers the alternated release of one electron from the whole system (Fe(II)Pc−$[N_2H_3]^-$) and then one proton from the electron donor species $[N_2H_3]^-$. Model 2 is based on two main steps, the alternated loss of two electrons from the system, and then the release of two protons from the

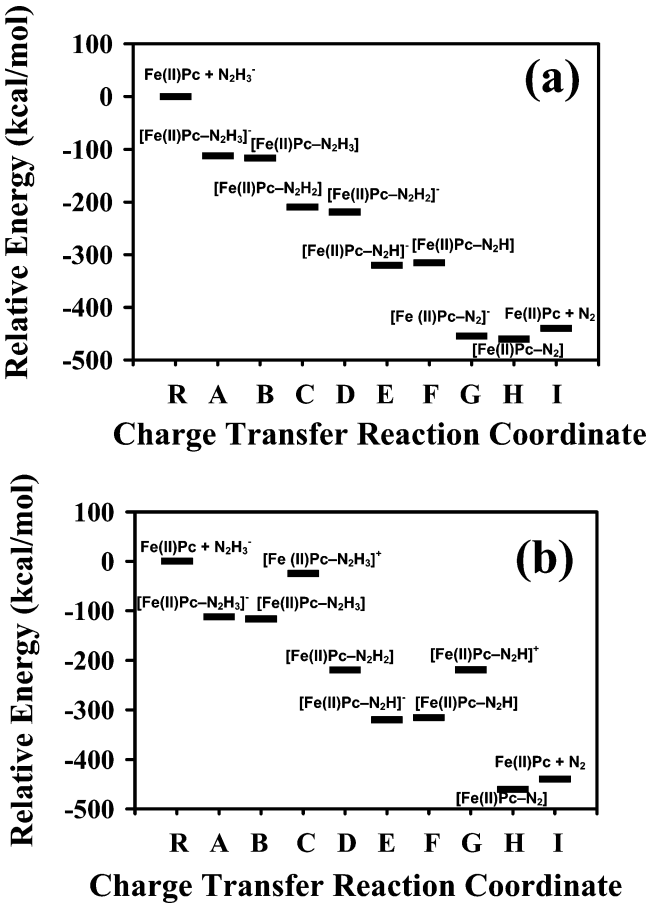

Figure 2. Total energy profiles for the hydrazine oxidation mechanism mediated by Fe(II)Pc: (a) model 1; (b) model 2. R: reactants (Fe(II)Pc and $N_2H_3^-$).

$[N_2H_3]^-$ residue. Both models end up in the full four-electron oxidation of anionic hydrazine to produce molecular nitrogen. Figure 2 shows the different steps for each model included in a total energy profile. The mass and charge equilibrium in each step were omitted for clarity purposes, considering only the species that undergo the redox and chemical changes. Nevertheless, in the analysis of the total energies associated with each reaction along the model, we have taken into account a complete mass and charge equilibrium.

We have investigated if a through-space charge-transfer mechanism occurs for the first electron transfer from the donor to the acceptor species, as we previously reported for the hydrazine oxidation by Co(II)Pc.[29c] We have previously shown that the spin density is a good descriptor for the electron transfer.[29] A spin density (ρ^s) scan using a reaction coordinate defined by the distance between the iron atom and one of the nitrogen atoms of hydrazine $r_{Fe\cdots N}$ from 3.0 to 6.0 Å did not show a through-space charge-transfer process. Therefore, our starting point was the optimized bonded [FePc−N_2H_3]$^-$ species.

We present the results in terms of three fragments: iron atom (Fe), macrocycle molecule (Pc), and hydrazine residue. Table 1 shows the total energy change given by $\Delta E = E$(products) − E(reactants), where E(products) and E(reactants) correspond to the sum of the total energy associated with all of the species present in the products and the reactants, as seen in Figure 2. We have also included in Table 1: (a) the electronic population change between consecutive steps, given by $\Delta\rho = \rho$(products) − ρ(reactants), where ρ(products) and ρ(reactants) correspond to the electronic populations of the three different fragments, and (b) the spin density values for each fragment.

TABLE 1: Variation of the Total Energy (ΔE) (kcal/mol), Electronic Population ($\Delta\rho$), and Spin Density (ρ^s) for Each Step of the Hydrazine Residue Oxidation Mechanism Mediated by Fe(II)Pc[a]

Model 1

		$\Delta\rho$			ρ^s		
step	ΔE	Fe	macrocycle	hydrazine residue	Fe	macrocycle	hydrazine residue
A	−112.300	0.030	0.600	−0.620			
B	−4.400	−0.195	−0.477	−0.328	0.702	0.060	0.283
C	−93.300	0.114	1.013	−1.127	0.024	0.975	0.001
D	−9.500	0.009	−0.963	−0.046			
E	−100.700	0.148	0.434	−0.581			
F	4.600	−0.248	−0.519	−0.232	0.809	0.065	0.125
G	−138.900	0.083	0.973	−1.056	0.020	0.979	0.000
H	−6.100	0.000	−0.967	−0.033			
I	20.600						

Model 2

		$\Delta\rho$			ρ^s		
step	ΔE	Fe	macrocycle	hydrazine residue	Fe	macrocycle	hydrazine residue
A	−112.300	0.030	0.600	−0.620			
B	−4.400	−0.195	−0.477	−0.328	0.702	0.060	0.283
C	92.400	0.018	−0.959	−0.060	0.642	1.056	0.302
D	−195.200	0.105	1.008	−1.113			
E	−100.700	0.148	0.434	−0.581			
F	4.600	−0.248	−0.519	0.232	0.809	0.065	0.125
G	96.500	0.014	−0.965	−0.049	0.797	1.065	0.138
H	−241.400	0.014	0.971	−0.881			
I	20.600						

[a] $\Delta E = E$(products) − E(reactants), where E(products) and E(reactants) correspond to the sum of the total energy associated with all of the species present for the products and the reactants of each step.

3.1.1. Model 1. In the above section, we have discussed why we proposed a pure through-bond charge-transfer mechanism for both models. Therefore, the starting point for both proposed mechanisms involves the interaction of Fe(II)Pc with the donor species to form a covalent adduct, $[FePc-N_2H_3]^-$ (see Figure 2).

The covalent species, $[FePc-N_2H_3]^-$, can be assigned as a singlet or triplet state. The singlet state is 2.90 kcal/mol more stable than the triplet state. Thus, the $[FePc-N_2H_3]^-$ species has a $\rho^s = 0.0$. On the other hand, the results of $\Delta\rho$ obtained for step A (see Table 1), which considers the difference between the electronic population of the $[FePc-N_2H_3]^-$ species with respect to the precursor species (Fe(II)Pc + $N_2H_3^-$), indicate that the hydrazine residue loses approximately 0.6e, which were transferred to the macrocycle. The latter indicates that when the electron-transfer process occurs, an electronic rearrangement through the Fe−N bond is produced, leading to a more stable structure with approximately 0.6e on the macrocycle instead of localized on the iron atom.

To continue with the redox process of the hydrazine, we removed one electron from the $[FePc-N_2H_3]^-$ system to produce the $[FePc-N_2H_3]$ neutral adduct (step B). The $[FePc-N_2H_3]$ species corresponds to a doublet state. The calculated spin densities give a value of 0.702 localized on the iron atom and a value of 0.283 for the hydrazine residue (Table 1, Figure 3a). The variation of the electronic population ($\Delta\rho$) between the $[FePc-N_2H_3]^-$ and $[FePc-N_2H_3]$ species is shown in Table 1. We found a value of −0.477 for the macrocycle and −0.328 for the hydrazine residues, indicating that these fragments present the major loss of electronic population when the neutral $[FePc-N_2H_3]$ is formed. The iron center shows an electronic density change of $\Delta\rho = -0.195$. In the previous study using the same methodology with CoPc,[24] we reported that the formation of the neutral $[CoPc-N_2H_3]$ species occurs with an electron loss mainly from the macrocyclic fragment ($\Delta\rho = -0.970$). In summary, in the first electron oxidation step, a different role of the metal atom for the two studied systems (Fe(II)Pc and Co(II)Pc) is observed.

The next step (step C) involves the loss of a proton from the $[FePc-N_2H_3]$ neutral species to form the anionic species $[FePc-N_2H_2]^-$. This species corresponds to a doublet state, with a spin density value of $\rho^s = 1$. The calculated ρ^s values for the fragments are presented in Table 1. From the obtained values, it is possible to observe that the unpaired electron is localized on the macrocycle fragment ($\rho^s = 0.975$). Table 1 also presents the calculated $\Delta\rho$ value associated with step C, which has a value of −1.127 for the hydrazine residue and 1.013 for the macrocycle fragment. From the obtained values, it is possible to infer that when the system loses the second proton, one electron is transferred from hydrazine residue to the macrocycle fragment through the Fe−N bond. The calculated $\Delta\rho$ value for the iron atom is 0.114, meaning that this metal does not experience a substantial change in step C. Furthermore, the above indicates that the next electron release will be occurring from the macrocycle fragment. Figure 3b shows the surface of the spin density for $[FePc-N_2H_2]^-$, indicating that the unpaired electron is localized on the macrocycle.

Step D involves the release of one electron out of the system to produce the neutral $[FePc-N_2H_2]$ species. This species could be assigned as a singlet or triplet state. The calculated energy for the singlet state is 29.9 kcal/mol more stable than the calculated one for the triplet state, and then $\rho^s = 0.000$. The calculated value for $\Delta\rho$ associated with step D is −0.963 for the macrocycle fragment, indicating that one electron has been released. The calculated values of $\Delta\rho$ for the iron atom and the hydrazine residue are nearly zero. We can conclude that the electron released in this step occurs through the macrocycle; this result is similar to that obtained for $[CoPc-N_2H_2]$ species ($\Delta\rho = -0.870$).

The next step (step E) involves the loss of one proton from the system leading to the formation of the anionic species $[FePc-N_2H]^-$. The calculated energy for the singlet state is 81.5

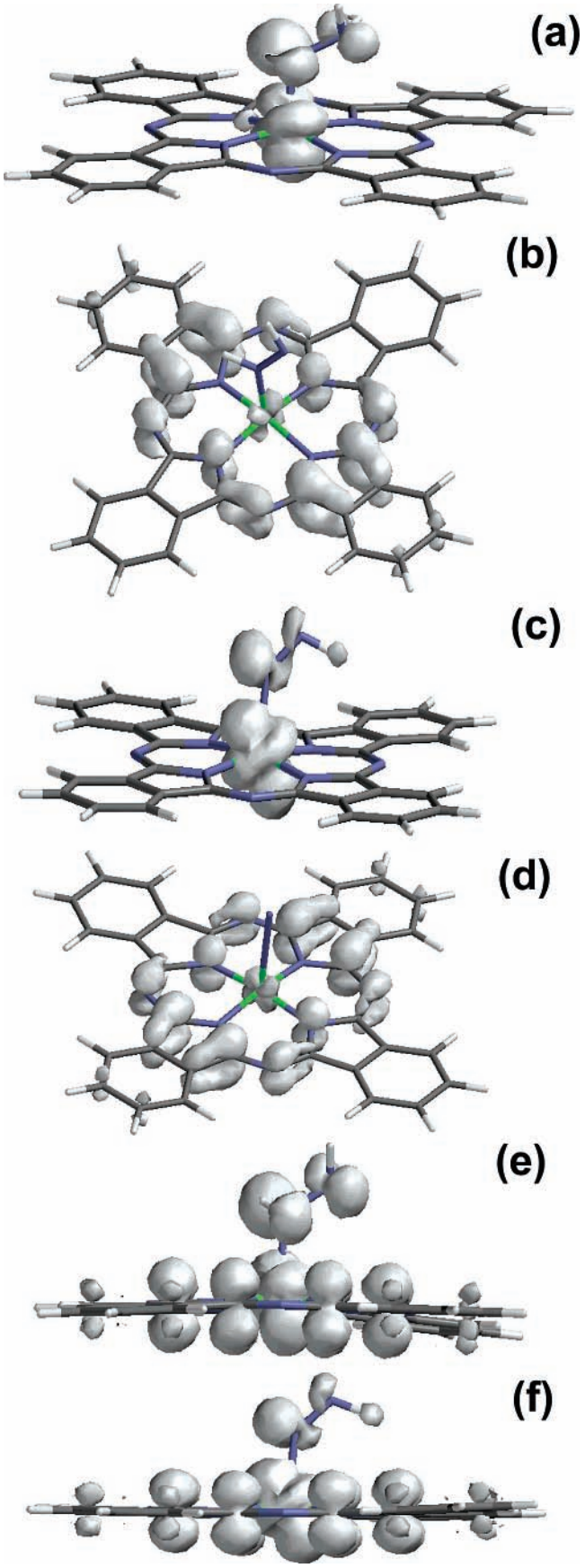

Figure 3. Spin density surfaces calculated at the B3LYP/LACVP(d) theory level of: (a) [FePc−N_2H_3]; (b) [FePc−N_2H_2]$^-$; (c) [FePc−N_2H]; (d) [FePc−N_2]$^-$; (e) [FePc−N_2H_3]$^+$; (f) [FePc−N_2H]$^+$.

kcal/mol more stable than that calculated for the triplet state, and therefore the anion will be assigned as a singlet state (ρ^s = 0.000). The calculated $\Delta\rho$ values indicate that the hydrazine residue transfers a total of 0.582e, that is, 0.434e to the macrocycle and 0.148e to the iron atom. This result is analogous to that obtained for the cobalt system where the calculated $\Delta\rho$ values show the same trend, that is, a larger electron transfer to the macrocycle fragment.

The next step (step F) involves the loss of an electron out of the system, leading to the formation of the neutral [FePc−N_2H] species. This neutral adduct corresponds to a doublet state, where the unpaired electron is mainly localized on the iron atom (ρ^s = 0.809) (see Figure 3c). The analysis of the calculated values for electronic population associated with step F shows that the electron was released mainly from the macrocycle fragment ($\Delta\rho$ = −0.519). As was shown in step B, the other fragments also participate in the electron release, $\Delta\rho$ = −0.248 for Fe atom and $\Delta\rho$ = −0.232 for hydrazine residue.

The last loss of one proton is shown in step G, which involves the formation of the anionic species [FePc−N_2]$^-$. The formed anion corresponds to a doublet state with the unpaired electron localized on the macrocycle (ρ^s = 0.979), as may be seen in Figure 3d. As in previous steps, the obtained results show a through-bond intramolecular electron transfer from the hydrazine residue ($\Delta\rho$ = −1.056) to the macrocycle ($\Delta\rho$ = 0.973).

These results indicate that the transferred electron produced by the oxidation of the hydrazine residue is better stabilized on the macrocycle fragment. The release of the transferred electron then occurs from the macrocycle fragment leading to the neutral [FePc−N_2] species (step H). This species presents a singlet state, and the calculated value for the electronic population shows that the release of the electron occurs from the macrocycle ($\Delta\rho$ = 0.967), which is a behavior similar to that calculated for step D.

3.1.2. Model 2. Model 2 differs from model 1 because the former considers the release of two consecutive protons, and then the release of two consecutive electrons, while model 1 considers the consecutive steps of one proton release and then one electron release. Besides, model 2 also considers cationic species.

The first two steps (steps A and B) are the same for both models; that is, step A takes into account the Fe(II)Pc and $N_2H_3^-$ interaction, and step B considers the first oxidation of the whole system. The third step (step C) involves the second electron release of the system from [FePc−N_2H_3], producing the cationic species [FePc−N_2H_3]$^+$ (see Figure 2). The calculated spin density for this system, which corresponds to a triplet state, is localized throughout the whole species, but mainly on the macrocycle (ρ^s = 1.056) and in a minor degree on the iron atom (ρ^s = 0.642) and on the hydrazine residue (ρ^s = 0.302) (see Figure 3e). The calculated $\Delta\rho$ values are indicative that the second electron release occurred from the macrocycle ($\Delta\rho$ = −0.959), in contrast with calculated values for step B where the loss of the electron occurred from the three fragments. Following the oxidation process of the hydrazine residue, the next two steps correspond to the loss of two protons (steps D and E, see Figure 2). The neutral [FePc−N_2H_2] species formed in step D corresponds to a singlet state (ρ^s = 0.000) and presents an intramolecular electron transfer from hydrazine ($\Delta\rho$ = −1.113) to the macrocycle ($\Delta\rho$ = 1.008), showing the oxidation of the hydrazine residue. Step E was already discussed in detail in section 3.1.1. The next two steps correspond to two successive electrons' release (steps F and G). Step F was already discussed in a previous section. Step G involves the formation of the

cationic species $[FePc-N_2H]^+$, which is a triplet state and shows the calculated spin density mainly on the macrocycle ($\rho^s = 1.065$) and on the iron atom ($\rho^s = 0.797$) (see Figure 3f). As occurred in step C, the electron release of step G occurred from the macrocycle fragment ($\Delta\rho = -0.965$). The last step (step H) is the release of the last proton of the system, leading to the neutral $[FePc-N_2]$ species with a singlet state ($\rho^s = 0.000$). The calculated $\Delta\rho$ values for the three fragments again show that an intramolecular electron transfer occurred, hydrazine residue lost 0.881e and the macrocycle fragment gained 0.971e, and therefore the oxidation process of hydrazine residue has been completed. The last step (step I) implies the rupture of the Fe−N bond and the formation of molecular nitrogen recovering the catalyst FePc.

In the previous section, we discussed the electron-transfer process in the oxidation of hydrazine mediated by Fe(II)Pc based on two different models only in terms of spin density and electronic population. From the energetic point of view, we also did an analysis of the calculated total energy values considering each step in both models, starting from the reactants Fe(II)Pc and $N_2H_3^-$ and ending with the formation of the products N_2 and Fe(II)Pc. Our results indicate that the energy difference between the reactants and the products is negative and about −440 kcal/mol, which is a spontaneous process. It is important to remark that the formation of cationic species ($[FePc-N_2H_3]^+$ and $[FePc-N_2H]^+$) in model 2 leads to a positive energy difference between the corresponding steps, and therefore those two steps are unfavorable from an energetic point of view (nonspontaneous processes).

3.2. Condensed to Atom Properties. In the previous section, we discussed the whole transfer process using charge-transfer descriptors such as electronic population and spin density based on different fragments. In this section, we analyze the oxidation sites of the adducts that present the remotion of one electron outside of the system. In the previous section, we found that in all cases (for the species that correspond) the electron is removed from the macrocycle. Now, using an orbital description such as the Fukui function, we will verify the above results. The Fukui function $f(r)$ is a well-known descriptor that allows one to identify the reactive sites.[45−47] $f(r)$ is an orbital descriptor and gives information about the softer sites in a molecule, which is of greater reactivity. We have demonstrated in previous works[48−50] that the determination of condensed Fukui functions from the molecular orbital point of view, that is, making use of the frontier molecular orbitals such as HOMO (highest occupied molecular orbital (MO)) and LUMO (lowest unoccupied molecular orbital), represents a well-accepted approximation. The latter are calculated from the electronic density of an MO ($\rho_{HOMO}(r)$,$\rho_{LUMO}(r)$), which is an observable and therefore has a physical meaning. In the present work, we also wanted to verify from the other point of view the external oxidation sites (remotion of one electron) of several of the proposed adducts participating in the charge-transfer mechanism. We calculated condensed Fukui functions ($f_{HOMO,k}$)[45−47] evaluated for the HOMO molecular orbital condensed to one atom or to a group of atoms that we called in the above section a fragment (k): macrocycle, hydrazine residue, and iron:

$$f_{HOMO,k} = \rho_{HOMO,k} = \sum_{i=1}^{N_k} (c_i^{HOMO,k})^2$$

where "i" represent the basis functions (atomic orbital) and N_k is the total number of basis functions of a given k. To determine which fragment presents a greater reactivity to an external oxidation process (outside of the system), we analyzed the values obtained for $f_{HOMO,k}$; that is, a higher value of $f_{HOMO,k}$ has the meaning of a greater reactivity.

TABLE 2: Fukui Functions Condensed to Different Fragments Evaluated on the HOMO Molecular Orbital Calculated at the B3LYP/LACVP(d) Level of Theory, for the Species That Participate in the Oxidation Mechanism of Hydrazine and Present the Remotion of One Electron

fragment	$f_{HOMO,k}$	fragment	$f_{HOMO,k}$
$[FePc-N_2H_3]^-$		$[FePc-N_2H_2]^-$	
macrocycle	0.10	macrocycle	0.82
hydrazine residue	0.59	hydrazine residue	0.01
Fe	0.25	Fe	0.03
$[FePc-N_2H]^-$		$[FePc-N_2]^-$	
macrocycle	0.07	macrocycle	0.82
hydrazine residue	0.55	hydrazine residue	0.00
Fe	0.30	Fe	0.03
$[FePc-N_2H_3]$		$[FePc-N_2H]$	
macrocycle	0.06	macrocycle	0.05
hydrazine residue	0.19	hydrazine residue	0.11
Fe	0.73	Fe	0.78

Table 2 shows the results obtained of $f_{HOMO,k}$ for six species that we proposed in the oxidation mechanism of hydrazine. For $[FePc-N_2H_3]^-$ (model 1), we found that $f_{HOMO,k}$ predicts the loss of one electron mainly on the hydrazine residue (0.59), in contrast to that obtained with electronic population ($\Delta\rho$) that the loss of one electron leading to $[FePc-N_2H_3]$ is divided between the macrocyle (−0.477) and the hydrazine residue (−0.328). The next species that presents an oxidation of one electron in model 1 corresponds to $[FePc-N_2H_2]^-$. $f_{HOMO,k}$ predicts that in this species the loss would occur mainly from the macrocycle (0.82), in agreement with the results of $\Delta\rho$ for step D from $[FePc-N_2H_2]^-$ to $[FePc-N_2H_2]$ (−0.963) where the electron is mainly released from the macrocycle. The third species that presents an external oxidation corresponds to $[FePc-N_2H]^-$, and the Fukui function predicts that the most probable site to present a loss of one electron is the hydrazine residue (0.55). Although $\Delta\rho$ does not predict exactly the same for step F corresponding to $[FePc-N_2H]^- \rightarrow [FePc-N_2H]$, we found that both descriptors, $f_{HOMO,k}$ and $\Delta\rho$, predict a similar trend, that the release of one electron from the system is shared between the fragments. The fourth external oxidation is analyzed for $[FePc-N_2]^-$, and $f_{HOMO,k}$ is predicted on the macrocycle (0.82) in full agreement with $\Delta\rho$ associated with the change $[FePc-N_2]^- \rightarrow [FePc-N_2]$ (−0.967). In model 2, the second release of one electron occurs in step C for the change from $[FePc-N_2H_3]$ to $[FePc-N_2H_3]^+$. $f_{HOMO,k}$ predicts that the oxidation site corresponds notoriously to the iron atom (0.73), a result that does not agree with that obtained using $\Delta\rho$, which predicts that the charge loss would come from the macrocycle (−0.959). The fourth external oxidation would occur for the $[FePc-N_2H]$ species, leading to the formation of $[FePc-N_2H]^+$ (step G). The results of $f_{HOMO,k}$ indicate that the oxidation of one electron would occur mainly from the iron atom (0.78), giving a result completely different from that obtained using $\Delta\rho$, which predicts that the elimination would occur on the macrocycle (−0.965).

In light of the obtained results, we can conclude that the prediction of oxidation sites, by using the Fukui function $f_{HOMO,k}$ condensed on the fragments of macrocycle, hydrazine residue, and iron, presents in some cases an agreement with the variation of the electronic density $\Delta\rho$. The agreement works very well when $f_{HOMO,k}$ is applied to the adducts where the electron that will be removed is mainly localized in one fragment and not scattered in several fragments. It is the case for the $[FePc-N_2H_2]^-$ and $[FePc-N_2]^-$ adducts. We attributed the differences

obtained between $f_{HOMO,k}$ and $\Delta\rho$ to the form of how the condensed Fukui functions were determined. The form used in this Article is approximated, and although in other work we have obtained very good results using $f_{HOMO,k}$,[48−50] all of them were applied to an isolated molecular structure, and not a supermolecule structure, as is the case here, an iron phthalocyanine coordinated to a hydrazine residue. As $f_{HOMO,k}$ was calculated from the highest occupied molecular orbital containing one or two electrons, depending on the adduct considered, there is no doubt that the results with $\Delta\rho$ are more accurate because they take into account all of the electrons of the adduct. Next, we conclude that, if $f_{HOMO,k}$ is used, it should not be used in an isolated way, but rather as a complement, and so the condensed Fukui function should be calculated in a more accurate form.

4. Conclusions

In this work, we showed that the theoretical model proposed to study the hydrazine oxidation mediated by Co(II)Pc reported in a previous work can also be applied to the same oxidation process mediated by Fe(II)Pc. We have also shown that the energy profile for the latter system is similar to that found for Co(II)Pc; that is, the oxidation process is energetically favorable.

In relation to the charge-transfer processes, we found that the first electron transfer occurs through bond (Fe−N) and not through space. Therefore, the four-electron oxidation process is governed by a through-bond charge-transfer mechanism.

The calculated electronic population values for steps involving the adduct oxidation (steps B−F, for both models) show a major participation of the metal center as compared to obtained results previously reported for the Co(II)Pc system. This major contribution of the metal center could explain the highest catalytic activity in the hydrazine oxidation observed at the experimental level for the Fe(II)Pc system in comparison with the Co(II)Pc system.

Finally, from a charge-transfer descriptor point of view, the spin density is a useful descriptor in the identification of the intramolecular charge transfer because it provides information of where the unpaired electron is localized. In contrast, electronic population and condensed Fukui function are very useful descriptors to recognize the molecular regions that are more sensitive to undergo an oxidation process, and hence they must be used in a complementary way. The latter descriptors show that the oxidation processes through the whole mechanism always involve more than one fragment or molecular region, verifying that both properties together could be used as good oxidation process descriptors.

Acknowledgment. We are thankful for financial support from Project FONDECYT Lineas Complementarias N° 8010006 and FONDECYT Regular N° 1060203 from CONICYT-Chile.

References and Notes

(1) Cook, L. J. *J. Mater. Chem.* **1996**, *6*, 677.
(2) Venkataraman, R.; Kunz, H. R.; Fenton, J. M. *J. Electrochem. Soc.* **2004**, *151*, A703.
(3) Kudrik, E. V.; Makarov, S. V.; Zahl, A.; van Eldik, R. *Inorg. Chem.* **2003**, *42*, 618.
(4) Zagal, J. H. *Coord. Chem. Rev.* **1992**, *119*, 89.
(5) Beck, F. *J. Appl. Electrochem.* **1977**, *7*, 328.
(6) Costamagna, J.; Canales, J.; Vargas, J.; Ferraudi, G. *Coord. Chem. Rev.* **1996**, *148*, 221.
(7) Zakharkin, G. I.; Tarasevich, M. R. *Electrokhimiya* **1975**, *11*, 1019.
(8) Radyushkina, K. A.; Tarasevich, M. R.; Akhundov, E. A. *Electrokhimiya* **1979**, *15*, 1884.
(9) Zagal, J. H.; Muñoz, E.; Ureta-Zañartu, S. *Electrochim. Acta* **1982**, *27*, 1373.
(10) Zagal, J. H.; Fierro, C.; Rozas, R. *J. Electroanal. Chem.* **1981**, *119*, 403.
(11) Yamada, K.; Yasuda, K.; Fujiwara, N.; Siroma, Z.; Tanaka, H.; Miyazaki, Y.; Kobayashi, T. *Electrochem. Commun.* **2003**, *5*, 892.
(12) Linares, C.; Geraldo, D.; Páez, M.; Zagal, J. H. *J. Solid State Electrochem.* **2003**, *7*, 626.
(13) Korfhage, K. M.; Ravichandran, K.; Baldwin, R. P. *Anal. Chem.* **1984**, *56*, 1514.
(14) Wang, J.; Pamidi, P. V. A.; Parrado, C.; Park, D. S.; Pingarron, J. *Electroanalysis* **1997**, *9*, 908.
(15) Ozoemena, K. I.; Nyokong, T. *Talanta* **2005**, *67*, 162.
(16) Li, X.; Zhang, S.; Sun, C. *J. Electroanal. Chem.* **2003**, *553*, 139.
(17) Huang, X. J.; Pot, J. J.; Kok, W. T. *Anal. Chim. Acta* **1995**, *300*, 5.
(18) Wang, J.; Naser, N. *Anal. Chim. Acta* **1995**, *316*, 253.
(19) Perez, E. F.; De Oliveira-Neto, G.; Tanaka, A. A.; Kubota, L. T. *Electroanalysis* **1998**, *10*, 111.
(20) Kubota, L. T.; Gushikem, Y.; Pérez, J.; Tanaka, A. A. *Langmuir* **1995**, *11*, 1009.
(21) Vinod, M. P.; Das, T. K.; Chandwadkar, A. J.; Vijayamohanan, K.; Chandwadkar, J. G. *Mater. Chem. Phys.* **1999**, *58*, 37.
(22) Peng, Q. Y.; Guarr, T. F. *Electrochim. Acta* **1994**, *39*, 2629.
(23) Zhang, J.; Tse, Y.; Pietro, W. J.; Lever, A. B. P. *J. Elelectroanal. Chem.* **1996**, *406*, 203.
(24) Zagal, J. H.; Lira, S.; Ureta-Zañartu, S. *J. Electroanal. Chem.* **1986**, *210*, 95.
(25) Geraldo, D.; Linares, C.; Cheng, Y. Y.; Ureta-Zañartu, S.; Zagal, J. H. *Electrochem. Commun.* **2002**, *4*, 182.
(26) Van der Putten, A.; Elzing, A.; Visscher, W.; Barendrecht, E. *J. Electroanal. Chem.* **1987**, *221*, 95.
(27) Zagal, J. H.; Páez, M.; Tanaka, A. A.; dos Santos, J. R.; Linkous, C. A., Jr. *J. Electroanal. Chem.* **1992**, *339*, 13.
(28) Cárdenas-Jirón, G. I.; Zagal, J. H. *J. Electroanal. Chem.* **2001**, *497*, 55.
(29) (a) Cárdenas-Jirón, G. I.; Venegas-Yazigi, D. *J. Phys. Chem. A* **2002**, *106*, 11938. (b) Venegas-Yazigi, D.; Cárdenas-Jirón, G. I.; Zagal, J. H. *J. Coord. Chem.* **2003**, *56*, 1269. (c) Paredes-García, V.; Cárdenas-Jirón, G. I.; Venegas-Yazigi, D.; Zagal, J. H.; Páez, M.; Costamagna, J. *J. Phys. Chem. A* **2005**, *109*, 1196.
(30) *IUPAC Compendium of Chemical Terminology*, 2nd ed.; 1996; Vol. 68, p 2280.
(31) (a) Felicissimo, V. C.; Cesar, A.; Luo, Y.; Gel'mukhanov, F.; Ågren, H. *J. Phys. Chem. A* **2005**, *109*, 7385. (b) Slowinski, K.; Chamberlain, R. V.; Miller, C. J.; Majda, M. *J. Am. Chem. Soc.* **1997**, *119*, 11910.
(32) Lee, C.; Yang, W.; Parr, R. G. *Phys. Rev.* **1988**, *B37*, 785.
(33) Miehlich, B.; Savin, A.; Stoll, H.; Preuss, H. *Chem. Phys. Lett.* **1989**, *157*, 200.
(34) Becke, A. D. *J. Chem. Phys.* **1993**, *98*, 5648.
(35) *TITAN 1.0.8*; Wavefunction, Inc. and Schrodinger Inc., 18401 Von Karman Avenue, Suite 370, Irvine, CA 92612.
(36) Weinhold, F.; Landis, C. R. *Chem. Ed.*: *Res. Pract. Eur.* **2001**, *2*, 91.
(37) Weinhold, F. *J. Chem. Educ.* **1999**, *76*, 1141.
(38) Foster, J. P.; Weinhold, F. *J. Am. Chem. Soc.* **1980**, *102*, 7211.
(39) Reed, A. E.; Curtiss, L. A.; Weinhold, F. *Chem. Rev.* **1988**, *88*, 899.
(40) Reed, A. E.; Weinhold, F. *J. Chem. Phys.* **1983**, *78*, 4066.
(41) Reed, A. E.; Weinstock, R. B.; Weinhold, F. *J. Chem. Phys.* **1985**, *83*, 735.
(42) Moliner, A. M.; Street, J. J. *J. Environ. Qual.* **1989**, *18*, 487.
(43) Golabi, S. M.; Zare, H. R. *J. Electroanal. Chem.* **1999**, *465*, 168.
(44) Razmi-Nerbin, H.; Pournaghi, M. H. *J. Solid State Electrochem.* **2002**, *6*, 126.
(45) Parr, R. G.; Yang, W. *J. Am. Chem. Soc.* **1984**, *106*, 4049.
(46) Yang, W.; Mortier, W. *J. Am. Chem. Soc.* **1986**, *108*, 5708.
(47) Chermette, H. *J. Comput. Chem.* **1999**, *20*, 129.
(48) Cárdenas-Jirón, G. I. *J. Phys. Chem. A* **2002**, *106*, 3202.
(49) Cárdenas-Jirón, G. I.; Parra-Villalobos, E. *J. Phys. Chem. A* **2003**, *107*, 11483.
(50) Ríos-Escudero, A.; Costamagna, J.; Cárdenas-Jirón, G. I. *J. Phys. Chem. A* **2004**, *108*, 7253.